Development and Measurement of the Jumping with Pneumatic Cylinder

Yun-Ju Chuang [1,*], Qinxin Zhan [2], and Ho Chang [3]

[1] Department of Mechanical Engineering, Minghsin University of Science and Technology (MUST), Taiwan
[2] College of Mechanical and Electrical Engineering, National Taipei University of Technology (NTUT), Taiwan
[3] Ph.D. Program in Semiconductor Technology, Minghsin University of Science and Technology (MUST), Taiwan
Email: andy2551468@gmail.com (Y.J.C.); q364849548@gmail.com (Q.Z.); hchang@must.edu.tw (H.C.)
*Corresponding author

***Abstract*—Jumping robots adopt an efficient locomotion strategy to overcome obstacles in competitive and unstructured environments. However, many existing designs rely on complex mechanisms with multiple degrees of freedom and sophisticated control algorithms, which limits their practicality in time-constrained applications. In this study, a lightweight single-degree-of-freedom jumping robot actuated by a pneumatic cylinder combined with elastic elements was developed. The design of the system and the results of an experimental evaluation are also discussed. The robot uses rubber bands for passive energy storage to enhance cylinder rebound and enable repeatable vertical jumping without complex control. A simplified dynamic model was developed to analyze the relationship between pneumatic force, elastic restoring force, and jumping performance. Experimental tests were conducted by varying the number of rubber bands to adjust the effective spring constant. The results demonstrate that using four rubber bands provides an optimal balance between rebound force and gas efficiency, and the robot achieved a maximum vertical jump height of 270 mm with a rebound cycle time of approximately 0.8 s. Configurations with fewer bands produced insufficient rebound force, whereas higher stiffness resulted in excessive air consumption. The findings confirm that pneumatic–elastic actuation can deliver efficient, stable, and repeatable jumping performance with minimal control complexity. Given its lightweight structure, inexpensive components, and ease of assembly, the proposed jumping robot offers a practical and resource-efficient solution for competition-oriented tasks and potential deployments in disaster relief scenarios where conventional robotic systems are limited.**

***Keywords*—jumping robot, pneumatic cylinder, vertical jump height, disaster relief**

I. Introduction

In this study, we establish a straightforward measurement methodology to evaluate the performance of robotic systems in jumping movements and utilize the measured results to enhance jumping capabilities. Jumping represents a unique and challenging mode of locomotion for robots. It provides an energy-efficient gait that can be a useful way to traverse complex or uneven terrain [1, 2]. In recent years, jumping tasks have frequently emerged in robotics competitions, which typically involve challenges such as overcoming single or multiple obstacles of varying heights [3].

Previous works on robotic jumping can generally be divided into two main categories. The first category of studies focused on robots with multiple Degrees of Freedom (DOF), which generally utilize rotary actuators to facilitate jumping through coordinated limb motions [4, 5]. Although such designs permit flexible motion and versatile gait planning, they frequently necessitate complex kinematic transformations requiring complex mechanical structures that tend to be difficult to maintain. This inherent complexity poses significant challenges in competitive environments, where limited preparation time and high operational demands leave little room for extensive repairs.

The second category is characterized by the development of jumping robots with a Single Degree of Freedom (SDOF) designed to execute unidirectional motion. These designs frequently incorporate pneumatic actuators in conjunction with elastic components to generate the required jumping force [6, 7]. Compared with multi-DOF robots, SDOF systems are characterized by a simpler structural design, ease of maintenance, and optimal suitability for competitions in which time is a critical factor. The exploitation of the energy storage and release properties of elastic materials enables the realization of efficient and repeatable jumping motions with minimal control complexity.

In this study, we integrate experimental investigations with engineering science principles to examine optimal jumping forces in terms of dynamics to satisfy the requirements specified by existing competitions. We propose that a control strategy may be developed to regulate the jumping force and the rebound speed of the cylinder to best meet the demands of competitions by analyzing the cylinder force, the elastic force provided by the rubber element, and the resulting spring-like rebound force. In particular, with regard to the control of the rubber

Manuscript received November 11, 2025; revised December 23, 2025; accepted February 3, 2026; published March 27, 2026.

force, we considered a robot equipped with a single pneumatic cylinder in conjunction with a rubber element. The control approach utilizes the energy storage and release characteristics of the rubber [8] to enable the system to accumulate and release energy to facilitate cylinder rebound. This strategy obviates the need for complex trajectory planning or intricate dynamic calculations [9].

To clarify the structure of our overarching research plan, we note that the present work constitutes the first phase of an ongoing investigation of pneumatically actuated jumping robots. In this preliminary stage, a deliberately simplified SDOF jumping robot was designed to eliminate ambiguous factors arising from complex mechanisms, multijoint coordination, and advanced control strategies. This simplification facilitated the identification and interpretation of the fundamental relationships between pneumatic force, elastic restoring force, air consumption, and jumping performance.

Therefore, the primary objective of this preliminary study was to establish a reliable experimental and analytical baseline to evaluate jumping performance rather than to maximize mechanical complexity or autonomy. Our results focus on the essential dynamics and performance trade-offs of pneumatic–elastic actuation, including the jumping height, rebound cycle time, and gas efficiency.

In subsequent phases of the research project, the design of the robot will be progressively expanded to encompass increased mechanical complexity, refined structural configurations, and more advanced control strategies. The experimental results obtained in this study will serve as reference benchmarks for comparison with future designs to support a systematic evaluation of how additional degrees of freedom, structural modifications, and control methods influence jumping performance.

II. Literature Review

A. Jumping Mechanisms for Legged and Monopod Robots

Jumping locomotion has been a central theme in legged robotics for a considerable period of time because it enables robots to traverse obstacles and execute highly dynamic maneuvers. Early studies on single-leg prototypes and simplified monopod models provided the foundation for established frameworks, such as the Spring-Loaded Inverted Pendulum (SLIP) model, which are still utilized for dynamic analysis and controller validation [10, 11]. These studies have highlighted the significance of monopod prototypes in the analysis of nonlinear hybrid dynamics during hopping and in the evaluation of control strategies prior to their implementation in quadrupeds or humanoids.

Recent experimental platforms demonstrated significant advancements in performance. For instance, the Salto-1P robot achieved extreme vertical jumping agility by combining lightweight structures, high-energy actuation, and optimized energy storage [12]. It has been demonstrated that mechanical design choices such as mass distribution, leg kinematics, and compliance directly influence the height to which a system can jump as well as repeatability and landing safety [13, 14]. This has been demonstrated by other designs, including monopods with reaction wheels. Surveys of bioinspired jumping robots have confirmed that to ensure robust operation, successful takeoff, aerial posture regulation, and landing buffering must be co-designed [15].

B. Pneumatic and Elastic Actuation for Hopping and Jumping

Pneumatic actuators are attractive for jumping robots because of their high power-to-weight ratio and relatively simple linear force outputs [16]. Their extensive utilization in the domain of competitive robots is attributable to the critical factors of simplicity, weight reduction, and high output force. Pneumatic cylinders with elastic materials such as rubber bands or springs have been integrated into these mechanisms to store energy to be released during the takeoff phase [17, 18]. The practical potential of combining pneumatic actuation with elastic energy recovery has been further illustrated by industrial prototypes such as Festo's Bionic Kangaroo [19].

Compliant actuation strategies have been proposed to overcome the limitations of pneumatic dynamics such as valve delay, pressure supply, and high air consumption. Series Elastic Actuators (SEAs) have been shown to decouple actuator dynamics from high-impact interactions to facilitate energy storage and enhanced force control [20]. This concept has been extended by robotic platforms that exploit carefully designed spring legs and SEAs to achieve a higher take-off power without excessively increasing the actuator torque requirements [21, 22]. Furthermore, analyses of different spring-linkage configurations have demonstrated that topology and force-deflection characteristics are critical in determining recoverable energy and efficiency [23].

C. Pneumatically Powered Jumping Robots

Pneumatically powered jumping robots exploit compressed air to generate high impulsive forces along with intrinsic mechanical compliance, which is beneficial for dynamic takeoff and impact mitigation. Compared with electrically actuated jumping robots, pneumatic systems—especially Pneumatic Artificial Muscles (PAMs)—offer higher power-to-weight ratios and muscle-like behavior, which makes them attractive for bio-inspired jumping and hopping mechanisms. Although general surveys of jumping robots include pneumatic actuation as a possible driving method, relatively few reviews of the relevant literature have focused on pneumatically powered jumping robots [15].

Most existing pneumatic jumping robots employ McKibben-type PAMs to mimic biological musculoskeletal systems. Early studies demonstrated that appropriate muscle arrangement and joint kinematics enable effective jumping motions in one-legged PAM-driven robots [24], whereas subsequent work investigated the coordinated pressure control of mono- and biarticular pneumatic muscles during the takeoff phase [25]. Bio-inspired designs, such as locust-like leg mechanisms and optimized knee joint geometries have

further shown that mechanical structure strongly influences jumping performance in PAM-driven systems [26, 27]. In addition to pure jumping platforms, pneumatic actuation has also been studied in legged robots designed to perform highly dynamic jumping motions. Antagonistic PAM-driven knee joints were modeled and controlled to reproduce fast, large-amplitude joint motions with compliance comparable to biological limbs [28], which provided important insights into pneumatic actuation under high dynamic loads. Moreover, jumping-related behaviors in legged robots, such as regulating posture in the flight phase, have been investigated in quadrupedal robots that perform long jumps, highlighting the importance of accurate control of joints during aerial phases [29]. These studies collectively indicate that although pneumatic actuation has demonstrated strong potential for jumping and jumping-related motions, unified modeling and control frameworks for pneumatically powered jumping robots remain underexplored.

D. Modeling, Optimization and Control Strategies for High-Performance Jumps

Jumping is an inherently hybrid and dynamic activity that requires precise control of contact timing, energy shaping, and trajectory optimization. In the context of quadrupeds, the employment of direct optimization and model predictive control methodologies has facilitated the calculation of feasible high-energy jumps while concurrently ensuring stability during landing [30, 31]. Research has indicated that optimal timing and whole-body coordination are more critical than leg force profiles alone in achieving reliable maneuvers [32].

For monopod robots, strategies such as bang-bang valve control for pneumatic cylinders, simple feedback triggers, and passive energy shaping have been applied to maximize energy release at the optimal moment [33, 34]. Energy-recovering landing mechanisms such as bistable or compliant structures reduce net power consumption and improve endurance for repeated hopping [35]. More recent developments have extended jumping to soft and compliant robots, including electroactive bistable jumpers and legless soft jumpers, which highlights the trade-off between efficiency and robustness across unstructured terrain [17, 36].

A comprehensive review of the relevant literature indicates that the integration of lightweight design, pneumatic–elastic actuation, and energy-optimized control strategies can result in a substantial enhancement of jump height and repeatability. Nevertheless, some notable challenge persists in balancing actuator limitations, energy efficiency, and robustness in real-world robotics competitions.

III. Materials and Methods

A. System Modeling and Dynamic Simulation

In this study, a jumping robot was designed with a lightweight structure consisting of three major components. The following elements were considered in the construction of the robot.

(1) A cushioning pad for vibration absorption during landing.
(2) An aluminum body to ensure both strength and low weight.
(3) A balloon-impact unit made of plastic to further reduce mass.

The pneumatic cylinder that functioned as the primary actuator was situated between the cushioning pad and robot body. A compact integrated cylinder was selected based on its ability to deliver sufficient output force to achieve a maximum jumping height of approximately 270 mm.

The jumping mechanism comprises six elements, including a gas tank, pressure gauge, three-way two-position valve, pneumatic cylinder, elastic bands, and a cushioning pad. Upon actuation of the valve, a flow of compressed air is initiated from the tank into the cylinder to generate the necessary force to propel the robot in an upward direction. The subsequent application of elastic bands is designed to provide a restoring force to ensure the retraction of the cylinder and subsequent actuation. The net jumping force is determined by subtracting the elastic restoring force from the cylinder force.

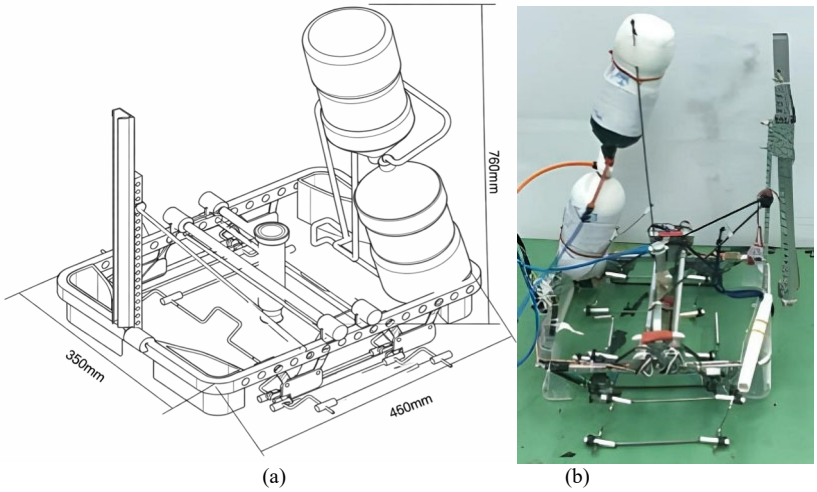

(a) (b)

Fig. 1. Design and prototype of the jumping robot. (a) Schematic diagram of the jumping robot in the competition; (b) Photograph of the jumping robot.

The competition-oriented jumping robots are illustrated in Fig. 1. Following the establishment of the robot's mathematical model, a sequential analysis of the three key factors affecting the jumping performance was conducted. The primary factor is the cylinder force, which generates the jumping propulsion. The second factor is the rebound speed of the cylinder, which is influenced by an elastic element (e.g., rubber). The third factor pertains to the regulation of gas consumption by air reservoirs.

We constructed a simplified model to investigate the dynamics based on three critical variables, including (i) cylinder output force, (ii) robot body mass, and (iii) the mass of the impact unit. The spring constants and damping coefficients corresponding to the models were incorporated into the simulation framework. The dynamic simulation is shown in Fig. 2.

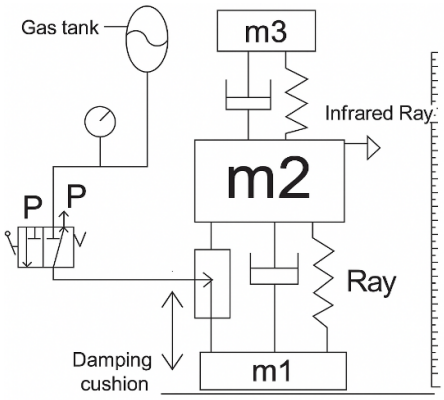

Fig. 2. The simulation dynamic graph.

B. System Modeling and Dynamic Simulation

A comparison was made between the theoretical model and physical measurements to validate the model experimentally. The experimental setup consisted of a jumping robot, an infrared height measurement system, and a calibrated ruler affixed to a vertical frame. The infrared sensor was mounted on the body of the robot, and its signal was continuously recorded throughout the tests.

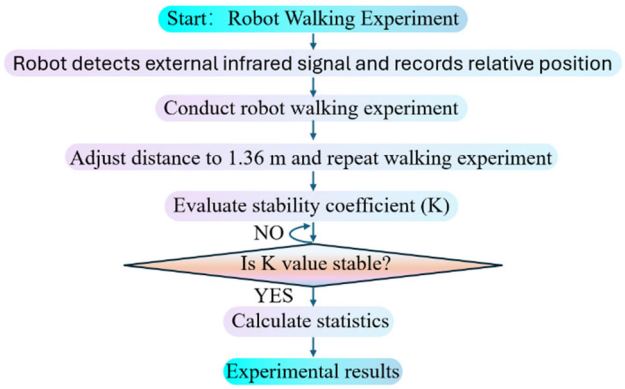

Fig. 3. The simulation dynamic graph.

The procedure was initiated by charging the pneumatic cylinder with compressed air, followed by actuation of the three-way valve to initiate the jump. A series of experiments was conducted in which the number of elastic bands was varied (from two to six) to enable the effective spring constant to be adjusted. Each configuration was subjected to repeated testing, and the resulting jump heights were recorded. The stepwise experimental process is illustrated in Fig. 3.

C. Force Calculation and Data Analysis

The net jumping force F is derived from the difference between the cylinder force (F_y) and the elastic restoring force F_e as given in Eq. (1):

$$F = F_y - F_e \tag{1}$$

The cylinder force is expressed as Eq. (2):

$$F_y = P \times A - m_1 a - F_\mu \approx P \times A, \tag{2}$$

where P is is the applied air pressure (2–4.5 atm), A is the cylinder piston area (14.52 mm^2), m_1 is the moving mass (negligible), and F_μ is the frictional force (negligible).

The elastic restoring force is calculated as Eq. (3):

$$F_e = k\delta, \tag{3}$$

where k is the spring constant (kgf/mm), determined by the number of elastic bands, and δ is the measured elongation (73 mm). With one elastic band, the effective spring constant was measured as 13.6 kgf/mm; adding bands increased the constant proportionally (e.g., two bands: 27.2 kgf/mm; six bands: 81.6 kgf/mm).

This approach allowed a systematic evaluation of the effect of spring stiffness on the required actuation pressure and resulting jump performance. Five test cases corresponding to different band counts were considered to produce comparative performance curves, as discussed in Section IV.

IV. Result and Discussion

Fig. 4. illustrates the determination of the spring constant using two rubber bands with k = 27.2 kgf/mm. The horizontal axis represents the adjustable pneumatic cylinder pressure (P), which ranges from 2 to 4.5 atm, whereas the vertical axis corresponds to the vertical jump height (mm), which reflects the jumping force F (N). The results indicated that the configuration with two rubber bands consumed the least amount of compressed gas; however, the cylinder rebound force was insufficient, which led to longer recovery times. Consequently, this configuration was deemed unsuitable for competitive applications.

When three rubber bands were applied, the corresponding spring constants were k = 40.8 kgf/mm (Fig. 5). Although the pneumatic cylinder pressure ranged from 2 to 4.5 atm and the vertical jump height was used as the performance indicator, the results demonstrated that the rebound force remained insufficient. The gas consumption was higher than that of the two-band case, further limiting its applicability to competition.

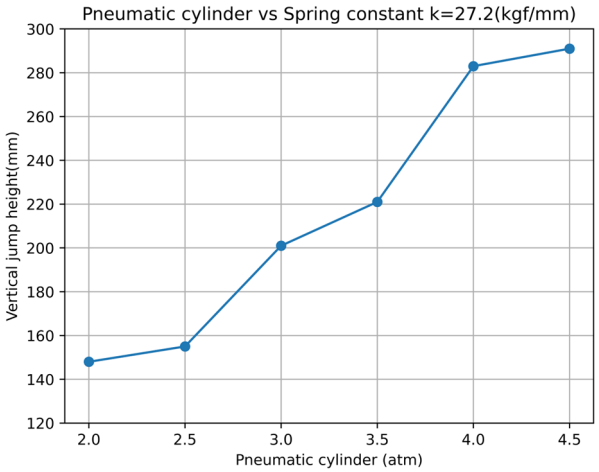

Fig. 4. The determination of the spring constant using two rubber bands.

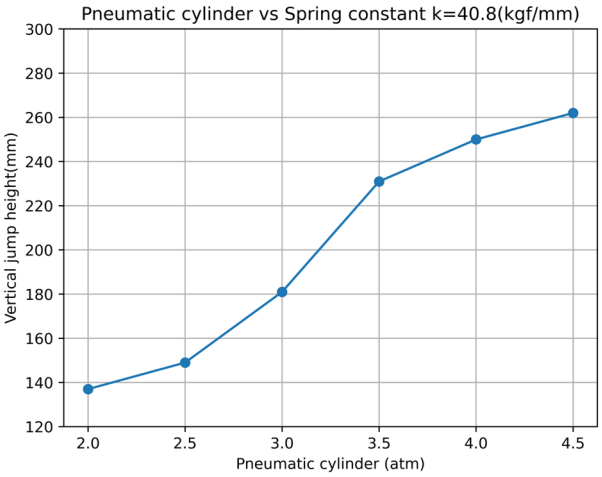

Fig. 5. The determination of the spring constant using three rubber bands.

Fig. 6 presents the results for the four rubber bands, yielding spring constants of k = 54.4 kgf/mm. This setup maintained gas consumption within the permissible range while providing a sufficient rebound force from the pneumatic cylinder. Among the tested conditions, this configuration was identified as the most suitable for competitive performance.

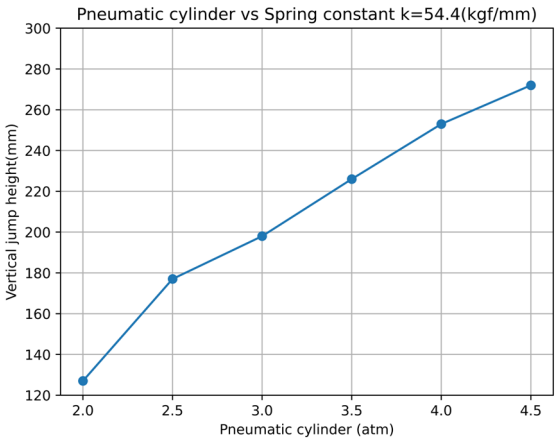

Fig. 6. The determination of the spring constant using four rubber bands.

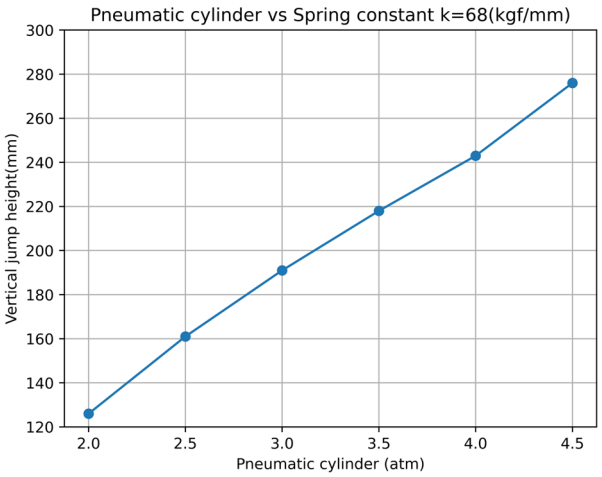

Fig. 7. The determination of the spring constant using five rubber bands.

In contrast, employing five rubber bands produced a spring constant of k = 68.0 kgf/mm (Fig. 7). Although gas consumption remained marginally within acceptable limits, it approached a critical threshold. Any operational error during the competition could render the system unable to perform subsequent jumps. Although the rebound force was sufficiently strong, the excessive risk of gas depletion rendered this setup impractical for competitive use.

When six rubber bands were used (spring constant k = 81.6 kgf/mm, Fig. 8), the gas consumption exceeded the allowable range. Despite generating a powerful rebound force, inefficient energy use disqualifies this configuration from being suitable for competition.

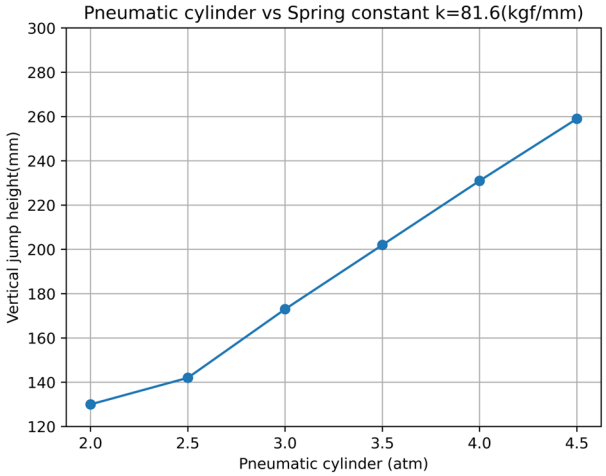

Fig. 8. The determination of the spring constant using six rubber bands.

Fig. 9 shows the overall performance of all five spring constants as a bar chart. The analysis clearly demonstrated that two and three rubber bands were insufficient because of the weak rebound forces and prolonged recovery times, whereas five and six rubber bands posed a risk of excessive gas consumption as noted. The configuration with four rubber bands achieved an optimal balance between rebound force and gas efficiency and thus provided the most competitive performance.

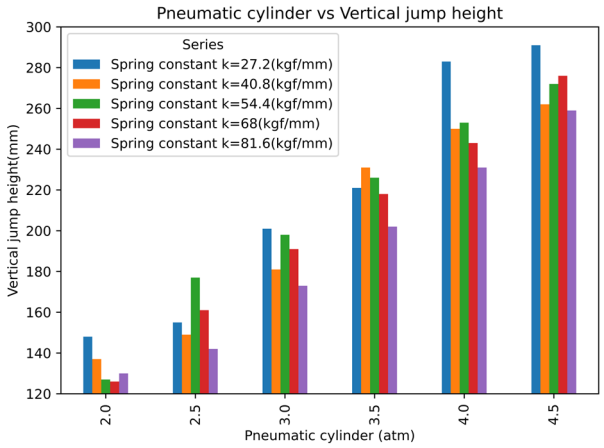

Fig. 9. Overall performance bar chart for five different spring constants.

Based on these findings, the proposed jumping robot utilizes elastic energy storage and release using rubber bands to enhance the rebound effect of a single pneumatic cylinder. By leveraging the natural resonance of the system, energy can be accumulated and efficiently converted into vertical jumping motion. This control method does not require complex trajectory planning or sophisticated dynamic computation. Instead, the actuation torque is directly provided by the pneumatic cylinder in combination with the elastic contribution of the rubber bands. This design approach enables back-drivability, which allows the mechanical structure to fully exploit its natural dynamics. The experimental validation confirmed that the robot was capable of continuous jumping with a sufficient rebound force. The maximum recorded vertical jump height was 270 mm, with a cylinder rebound cycle time of 0.8 s. Thus, the proposed configuration demonstrated excellent suitability for competition-oriented applications.

Table I summarizes the quantitative relationship between the elastic stiffness, jumping height, rebound cycle time, and air consumption for all tested configurations. As the effective spring constant increased, jump height and rebound speed improved; however, this was accompanied by a rapid increase in air consumption. Configurations with inadequate stiffness (two and three rubber bands) exhibited deficient rebound forces and protracted cycle times, whereas excessively rigid configurations (five and six rubber bands) resulted in increased gas usage, tending to impede repeatability.

TABLE I. SUMMARY OF JUMPING PERFORMANCE UNDER DIFFERENT ELASTIC CONFIGURATIONS

Number of Rubber Bands	Spring Constant k (kgf/mm)	Max Jump Height (mm)	Rebound Cycle Time (s)	Relative Air Consumption
2	27.2	Low (<200)	Long (>1.2)	Low
3	40.8	Moderate (~220)	Long (~1.0)	Moderate
4	54.4	270	0.8	Moderate (Optimal)
5	68.0	High	Short	High
6	81.6	High	Short	Excessive

The configuration using four rubber bands achieved an optimal tradeoff between jump height, cycle time, and air efficiency. The results of this quantitative comparison enhance the clarity of the performance trends and support the conclusion that moderate elastic stiffness is essential for efficient and repeatable pneumatic jumping.

V. CONCLUSION

In this study, we developed and experimentally validated a jumping robot actuated using a pneumatic cylinder in combination with elastic elements. Our results demonstrated that an optimal balance between spring constant and air consumption can be achieved by employing four rubber bands. The proposed configuration yields a stable rebound force, efficient energy conversion, and reliable vertical jumping performance, with a maximum recorded jump height of 270 mm. These results confirm the feasibility of using simple pneumatic–elastic actuation strategies to achieve repeatable and competition-ready robotic jumps without complex control algorithms or sophisticated hardware.

In the absence of a robotic competition context, the design philosophy of this study demonstrates more extensive applicability in real-world scenarios, including search and rescue operations, in the aftermath of disasters. The robot's lightweight structure, reliance on pneumatic actuation, and use of readily available elastic materials such as rubber bands and air tanks contribute to its high adaptability for rapid deployment in environments where conventional equipment is scarce. The ease of assembly and inexpensive components further support its implementation in the field during emergencies.

In summary, the proposed jumping robot is a robust and resource-efficient platform that combines mechanical simplicity and functional agility. These findings provide a quantitative framework for the optimization of pneumatic–elastic jumping systems. Furthermore, the proposed approach provides a promising pathway for the development of disaster-relief robots capable of overcoming obstacles in complex terrain using locally available and easily assembled materials.

CONFLICT OF INTEREST

The authors declare no conflicts of interest.

AUTHOR CONTRIBUTIONS

YJC conceived and designed the experiments, performed the primary writing of the manuscript, and revised it for important intellectual content; QZ was responsible for robot fabrication, data collection, sample analysis, and figure preparation; HC provided research advice and expertise; all authors had approved the final version.

REFERENCES

[1] Q. Zheng, X. Zhu, B. Wang *et al.,* "Ramp jump control of single-track two-wheeled robot using reinforcement learning with demonstration data," in *Proc. 2022 IEEE International Conf. on Robotics and Biomimetics (ROBIO)*, 2022, pp. 1769–1774.

[2] A. Beck, V. Zaitsev, U. B. Hanan *et al.,* "Jump stabilization and landing control by wing-spreading of a locust-inspired jumper," *Bioinspiration & biomimetics,* vol. 12, no. 6, 066006, 2017.

[3] J. Mo, Z. Yan, B. Li *et al.,* "Study of obstacle-crossing and pitch control characteristic of a novel jumping robot," *Sensors,* vol. 21, no. 7, 2432, 2021.

[4] P. Razzaghi, E. A. Khatib, and Y. Hurmuzlu, "Nonlinear dynamics and control of an inertially actuated jumper robot," *Nonlinear Dynamics,* vol. 97, no. 1, pp. 161–176, 2019.

[5] K. Arikawa and T. Mita, "Design of multi-DOF jumping robot," in *Proc. 2002 IEEE International Conf. on Robotics and Automation (Cat. No. 02CH37292)*, 2002, vol. 4, pp. 3992–3997.

[6] M. Kovač, M. Schlegel, J.-C. Zufferey *et al.,* "Steerable miniature jumping robot," *Autonomous Robots,* vol. 28, no. 3, pp. 295–306, 2010.

[7] Y. Chi, Y. Hong, Y. Zhao *et al.,* "Snapping for high-speed and high-efficient butterfly stroke–like soft swimmer," *Science Advances,* vol. 8, no. 46, eadd3788, 2022.

[8] C.-Y. Chan and Y.-C. Liu, "Towards a walking, turning, and jumping quadruped robot with compliant mechanisms," in *Proc. 2016 IEEE International Conf. on Advanced Intelligent Mechatronics (AIM)*, 2016, pp. 614–620.

[9] T. Guo, J. Liu, H. Liang *et al.*, "Design and dynamic analysis of jumping wheel-legged robot in complex terrain environment," *Frontiers in Neurorobotics,* vol. 16, 1066714, 2022.

[10] A. Sayyad, B. Seth, and P. Seshu, "Single-legged hopping robotics research—A review," *Robotica,* vol. 25, no. 5, pp. 587–613, 2007.

[11] Z. Xu, T. Lü, and F. Ling, "Trajectory planning of jumping over obstacles for hopping robot," *Journal of the Brazilian Society of Mechanical Sciences and Engineering,* vol. 30, pp. 327–334, 2008.

[12] D. W. Haldane, J. K. Yim, and R. S. Fearing, "Repetitive extreme-acceleration (14-g) spatial jumping with Salto-1P," in *Proc. 2017 IEEE/RSJ International Conf. on Intelligent Robots and Systems (IROS)*, 2017, pp. 3345–3351.

[13] A. Anzai, T. Doi, K. Hashida *et al.,* "Monopod robot prototype with reaction wheel for hopping and posture stabilisation," *International Journal of Mechatronics and Automation,* vol. 8, no. 4, pp. 163–174, 2021.

[14] L. Bai, F. Zheng, X. Chen *et al.,* "Design and experimental evaluation of a single-actuator continuous hopping robot using the geared symmetric multi-bar mechanism," *Applied sciences,* vol. 9, no. 1, 13, 2018.

[15] Z. Zhang, J. Zhao, H. Chen *et al.,* "A survey of bioinspired jumping robot: Takeoff, air posture adjustment, and landing buffer," *Applied bionics and biomechanics,* vol. 2017, no. 1, 4780160, 2017.

[16] P.-B. Wieber, R. Tedrake, and S. Kuindersma, "Modeling and control of legged robots," in *Springer Handbook of Robotics,* Springer International Publishing, 2016, pp. 1203–1234.

[17] D. Li, D. Niu, G. Ye *et al.*, "Crawling–jumping synergic bioinspired robots harnessing electroactive bistable actuators by adjusting mechanical responses and forces," *Applied Materials Today,* vol. 24, 101091, 2021.

[18] D. Guo and Z. Kang, "Chamber layout design optimization of soft pneumatic robots," *Smart Materials and Structures,* vol. 29, no. 2, 025017, 2020.

[19] K. Graichen and S. Hentzelt, "A bi-level nonlinear predictive control scheme for hopping robots with hip and tail actuation," in *Proc. 2015 IEEE/RSJ International Conf. on Intelligent Robots and Systems (IROS)*, 2015, pp. 4480–4485.

[20] G. A. Pratt and M. M. Williamson, "Series elastic actuators," in *Proc. 1995 IEEE/RSJ International Conf. on Intelligent Robots and Systems. Human Robot Interaction and Cooperative Robots*, 1995, vol. 1, pp. 399–406.

[21] D. W. Haldane, M. M. Plecnik, J. K. Yim *et al.*, "Robotic vertical jumping agility via series-elastic power modulation," *Science Robotics,* vol. 1, no. 1, eaag2048, 2016.

[22] M. Chignoli and S. Kim, "Online trajectory optimization for dynamic aerial motions of a quadruped robot," in *Proc. 2021 IEEE International Conf. on Robotics and Automation (ICRA)*, 2021, pp. 7693–7699.

[23] J. Lo and B. Parslew, "Elastic energy storage of spring-driven jumping robots," arXiv Preprint, arXiv: 2311.02188, 2023.

[24] Y. Yamamoto, H. Nishi, Y. Torii *et al.*, "Mechanism and jumping pattern of one-legged jumping robot with pneumatic actuators," in *Proc. 2016 16th International Conf. on Control, Automation and Systems (ICCAS)*, 2016, pp. 1132–1136.

[25] Y. Ishiyama, Y. Yamamoto, A. Takanishi *et al.*, "Jumping motion control of one-legged jumping robot with pneumatic muscles," in *Proc. 2018 18th International Conf. on Control, Automation and Systems (ICCAS)*, 2018, pp. 225–230.

[26] J. Zhong, C. Zhao, and H. Su, "A novel locust-inspired jumping robot driven by pneumatic muscle actuators," in *Proc. 2018 7th International Conf. on Energy and Environmental Protection (ICEEP 2018)*, 2018, pp. 1732–1735.

[27] T. Okumura, D. Nakanishi, K. Naniwa *et al.*, "Relationship between the shape of the elliptical knee joint and jumping height in a leg-type robot driven by pneumatic artificial muscle," *ROBOMECH Journal,* vol. 10, no. 1, 10, 2023.

[28] J. Magdy, O. M. Shehata, H. A. Kandil *et al.*, "Hybrid modelling, control and simulation of knee joint actuated by antagonistic pneumatic artificial muscles," *International Journal of Mechanical Engineering and Robotics Research,* vol. 14, no. 4, 2025.

[29] B. Bahceci, O. K. Adak, and K. Erbatur, "Push recovery of a quadrupedal robot in the flight phase of a long jump," *International Journal of Mechanical Engineering and Robotics Research,* vol. 11, no. 7, pp. 486–493, 2022.

[30] J. Schulman, J. Ho, A. X. Lee *et al.*, "Finding locally optimal, collision-free trajectories with sequential convex optimization," in *Proc. Robotics: Science and Systems*, Berlin, 2013, vol. 9, no. 1, pp. 1–10.

[31] G. Xin and M. Mistry, "Optimization-based dynamic motion planning and control for quadruped robots," *Nonlinear Dynamics,* vol. 112, no. 9, pp. 7043–7056, 2024.

[32] C. Nguyen and Q. Nguyen, "Contact-timing and trajectory optimization for 3d jumping on quadruped robots," in *Proc. 2022 IEEE/RSJ International Conf. on Intelligent Robots and Systems (IROS)*, 2022, pp. 11994–11999.

[33] C. Hong, D. Tang, Q. Quan *et al.*, "Energy-recoverable landing strategy for small-scale jumping robots," *Robotics and Autonomous Systems,* vol. 176, 104696, 2024.

[34] Y. Sugiyama and S. Hirai, "Crawling and jumping by a deformable robot," *The International Journal of Robotics Research,* vol. 25, no. 5–6, pp. 603–620, 2006.

[35] R. Chen, Z. Yuan, J. Guo *et al.*, "Legless soft robots capable of rapid, continuous, and steered jumping," *Nature Communications,* vol. 12, no. 1, 7028, 2021.

[36] A. B. Silva, M. Murcia, O. Mohseni *et al.*, "Design of low-cost modular bio-inspired Electric–Pneumatic Actuator (EPA)-driven legged robots," *Biomimetics,* vol. 9, no. 3, 164, 2024.